Journal of the European Ceramic Society **18** (1998) 269–274

PII: S0955-2219(97)00121-0
0955-2219/98/$19.00 + 0.00

The Effect of Impact Angle on the Erosion Rate of Polycrystalline α-Al_2O_3

A. Franco and S. G. Roberts

Department of Materials, University of Oxford, Parks Road, Oxford, UK, OX1 3PH

(Received 16 December 1996; accepted 16 June 1997)

Abstract

Wet erosive wear tests with SiC particle impacts at 45°, 60°, 75° and 90° were performed on polycrystalline α-Al_2O_3 specimens of mean grain size 1·2, 3·8 and 14·1 μm. The erosion rate was found to be strongly dependent on impact angle, being three to four times greater for impacts at 90° than for 45° impacts. The erosion rate varied strongly with grain size; the coarse grained material had erosion rates about six times greater than those of the finest grained material. The worn areas due to impacts after short erosion times were examined by SEM to characterise the erosion mechanisms; the mechanism of erosive wear appears to be by the interaction of the cracks from adjacent impacts. The variation of erosion rates with impact angle for all grain sizes showed a power law dependence on normal impact velocity, with an exponent of ~3·9. © *1997 Elsevier Science Limited.*

1 Introduction

In erosion of brittle materials, particle impacts cause brittle fracture. The intersection of cracks with each other and with the surface leads to material removal.[1] In many cases the impact-induced fracture is on a scale comparable to the dimensions of the particles causing the erosion.[2–6]

It is known that erosion of brittle and ductile materials has a strong dependence on the impact angle.[7] For brittle materials, the erosion rate decreases markedly as the impact angle decreases from 90° (i.e. normal to the eroded surface), while for ductile materials the erosion rate has a maximum at shallow impact angle, typically 20–30°.

The erosion rate of polycrystalline alumina has been found to be strongly dependent on grain size. In both dry erosion[6] and wet erosion[8,9] the erosion rate increases with grain size. For wet erosion the wear rate is about one order of magnitude greater for Al_2O_3 of a coarse grain size ($G = 14{\cdot}1\ \mu m$) than for Al_2O_3 of a fine grain size ($G = 1{\cdot}2\ \mu m$).[8,9] The erosion rates per impacting particle in the study of Miranda-Martinez *et al.*[8] were about 4–10 times lower than those of Franco and Roberts.[9] This difference was attributed chiefly to the effects of impacting angle: in the study of Franco and Roberts[9] the impacting angle was always 90° while in that of Miranda-Martinez *et al.*[8] the impact angle was not controlled and probably ranged from 45° to 90°.

In this paper we report the results of wet erosive wear testing of polycrystalline alumina specimens of three grain sizes ($G = 1{\cdot}2$, 3·8 and 14·1 μm) with varying impact angle. Impacts were produced at 45°, 60°, 75° and 90° angles, at a particle velocity ~2·4 ms^{-1}, using an erosive medium of SiC grits (mean size ~780 μm) in water. The erosion experiments were performed using the apparatus described by Franco and Roberts.[9]

2 Experimental Procedure

2.1 Sample fabrication

Near fully-dense polycrystalline alumina materials were fabricated using high purity, 99·9%, α-Al_2O_3 powder (Sumitomo AKP-50, Japan) of mean particle size ~180 nm. Alumina specimens of grain size 1·2 μm (referred to later as *F*) were produced by hot-pressing; specimens of grain size 3·8 μm and 14·1 μm (referred to later as *M* and *C*, respectively) were produced by pressureless sintering. Full details of the processing methods are given by Franco and Roberts.[9]

2.2 Wet erosive wear tests

The specimens were cut into bars of 10×10×5 mm. These were mechanically ground with 14 μm SiC slurry, polished on cloths impregnated with 6 μm polycrystalline diamond and finished with a 'Syton' polish. The testing medium consisted of 1·5 kg of

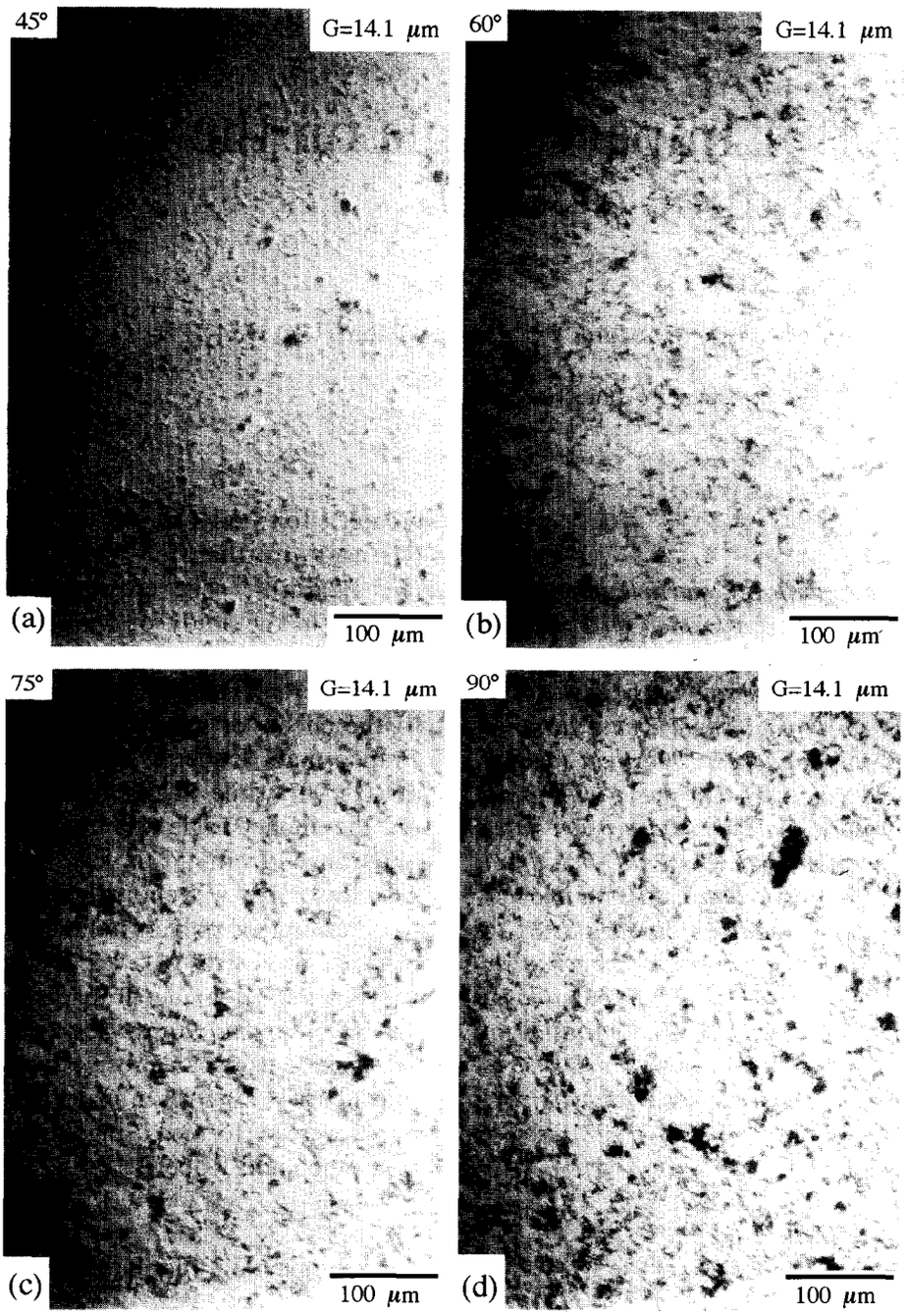

Fig. 1. Optical micrographs of eroded areas of polycrystalline alumina, $G = 14{\cdot}1\ \mu m$, due to impacts at (a) 45°, (b) 60°, (c) 75° and (d) 90°. Test time 1 min.

SiC grits* (Fig. 3(b) in Franco and Roberts[9]) with a mean size of $\sim 780\ \mu m$ and a mean mass of $9{\cdot}1 \times 10^{-4}$ g, dispersed in 8 litre of water. The velocity of particle impacts was determined by performing erosion tests on OHFC copper, and calibrating the results against a model based on the balance between the kinetic energy of spherical particle and the work of quasi-static indentation of a spherical indenter to produce the same impact crater depth. The calibration method gives the normal impact velocity solely as a function of the crater depth produced by impacts.[9,10] The impact velocity† was $2{\cdot}4 \pm 1{\cdot}5\ ms^{-1}$. The particle flux was determined by collecting all grit particles passing through the sample holder in a short test, and by measuring the impact area on the test specimens. The flux was found to be $8{\cdot}6 \times 10^7$ particles $m^{-2}s^{-1}$ for impacts at 90°.

For impacts at 45°, 60° and 75° the specimens were sliced from the corners and positioned on the

*SiC grits (type 24 C6) were provided by Washington Mills, Electro Mineral Ltd, Mosley Road, Trafford Park, Manchester, UK, M17 1NR.

†The impact velocity was incorrectly reported by Franco and Roberts[9] as $2{\cdot}7\ ms^{-1}$. This was due to a mistake in the calibration procedure; we are grateful to Dr I.M. Hutchings for finding the error.

sample holder in a way that impacts occurred at the desired angle. Tests performed were of two types: short tests (1 min) to produce surfaces on which the erosive damage processes could be inspected, and long tests (60, 120 and 360 min) to measure the weight losses and thus erosion rates.

The erosion rate, R, was calculated as:

$$R = \frac{\Delta\omega}{A_{\text{imp}}\rho\Delta t} \tag{1}$$

where $\Delta\omega = \omega - \omega_0$. ω_0 is the specimen weight before testing and ω is the specimen weight after testing for a time Δt. A_{imp} is the impact area and ρ is the specimen density. The erosion rate per particle, $\Re$, was calculated by dividing the erosion rate, R, by the impact flux (with impact areas corrected to those normal to the particle flux for $\theta \neq 90°$).

3 Results and Discussion

Figure 1 shows eroded areas of coarse grained polycrystalline alumina specimens ($G = 14{\cdot}1\ \mu$m) after 1 min of testing. Damage becomes more severe as the impact angle increases from 45° to 90°. Details of microfracture events characteristic of each impact angle are shown in Fig. 2. For

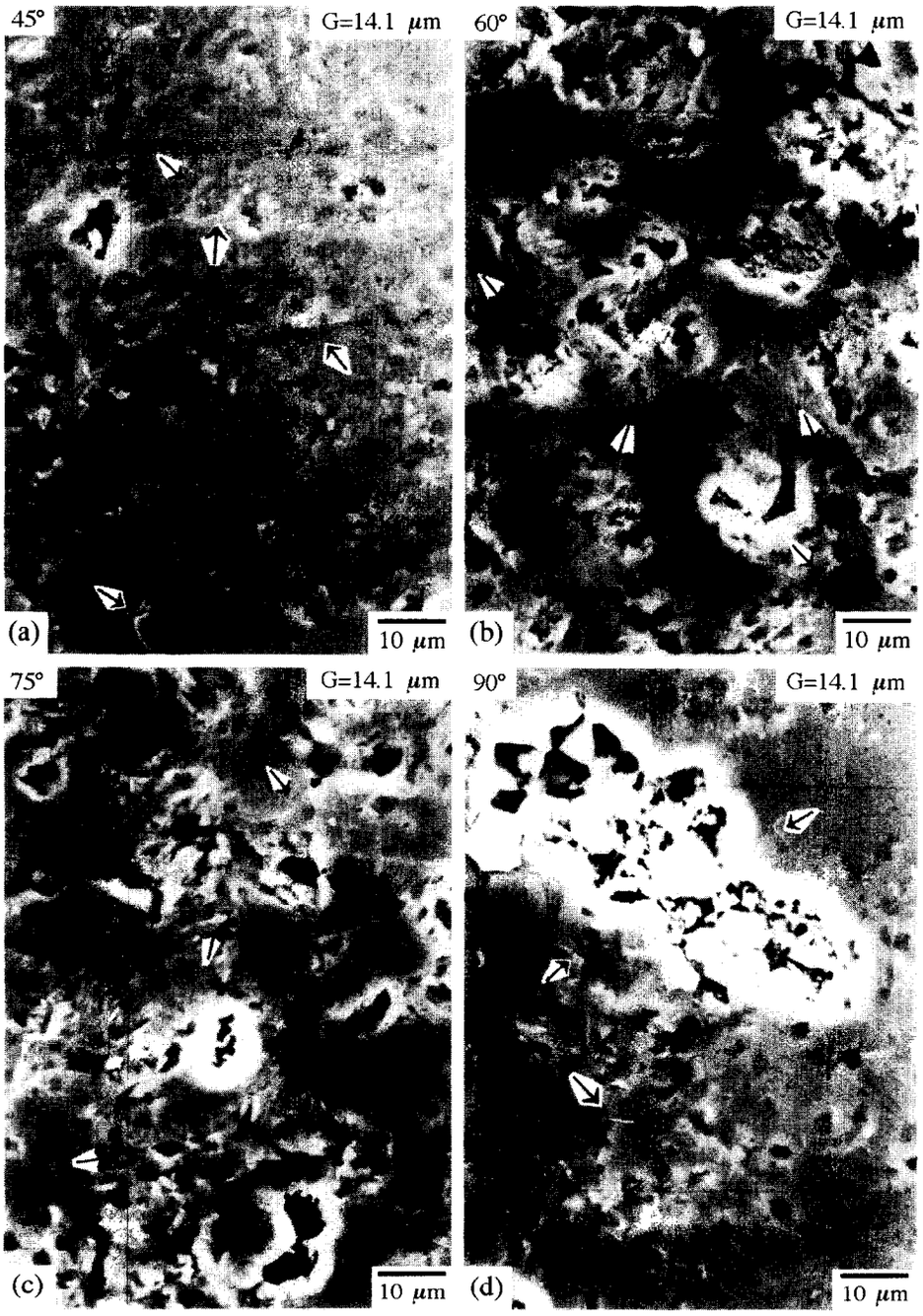

Fig. 2. SEM micrographs of eroded areas of polycrystalline alumina, $G = 14{\cdot}1\ \mu$m, due to impacts at (a) 45°, (b) 60°, (c) 75° and (d) 90°. Note presence of small cracks (see arrows) in all worn surfaces. Test time 1 min.

impacts at 45°, Fig. 2(a), the damage is quite mild and the scars are shallow impressions which are similar to those produced by 'machining' or scratching. In some areas it appears that material has been displaced or removed by plastic deformation. Small cracks are present (see arrows) and also there is evidence that grains have been detached. For impacts at 60°, Fig. 2(b), and 75°, Fig. 2(c), the damage is still mild but the scars are much bigger and similar to those produced by 'machining'. In some areas, cracks associated with damage zones are much more interconnected then those due to impacts at 45°. Small cracks are present and some grains have been detached. For impacts at 90°, Fig. 2(d), damage is more severe and the scars are similar to those produced by a sharp indenter. Small cracks are present and in some areas there is much brittle fracture. In all cases, large amounts of material are removed from the surface only where two or more impact sites are close to each other, so that the crack systems from the impact events intersect.

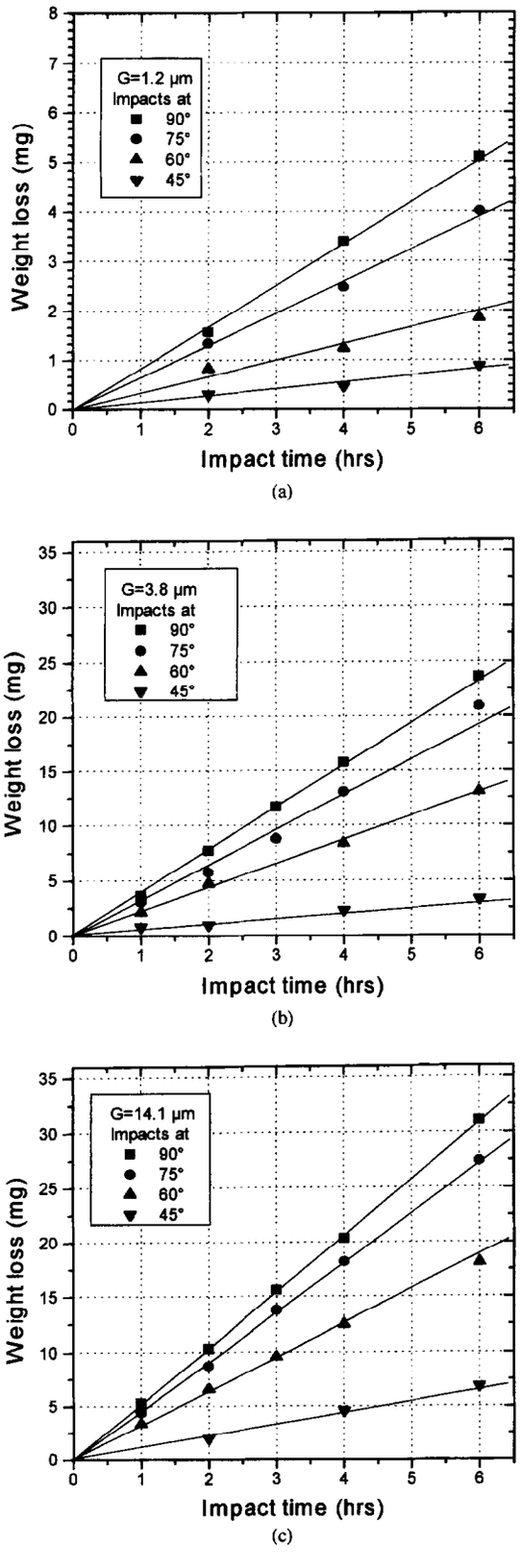

Fig. 3. Weight loss as a function of impact time for each impact angle. (a) $G=1{\cdot}2\,\mu$m, (b) $G=3{\cdot}8\,\mu$m and (c) $G=14{\cdot}1\,\mu$m.

Figure 3 shows weight loss versus erosion time for the three materials tested. The weight loss increases linearly with impact time and varies strongly with grain size and impact angle. Figure 4 shows the erosion rate per particle, $\Re$, versus impact angle and Table 1 summarises the erosion test results (impact areas, A_{imp}, mean weight loss, ω_{mean}, mean erosion rate, R_{mean}, and mean erosion rate per particle, $\Re_{mean}$). The erosion rate per particle is about three or four times greater for impacts at 90° then for impacts at 45°.$\Re$ is about six times greater for Al_2O_3 of 14·1 μm grain size than for the 1·2 μm grain size material.

Figure 5 plots the logarithm of erosion rate per particle versus the logarithm of the normal component of the impacting velocity for each incidence angle. The data for each grain size are a good fit to a straight line, implying a power law dependence of erosion rate on the normal component of the impact velocity. The slopes of the lines for each grain size are very nearly the same: F, 3·96; M, 3·87; C, 3·78. These values are similar to, but somewhat higher than, those predicted by a dynamic

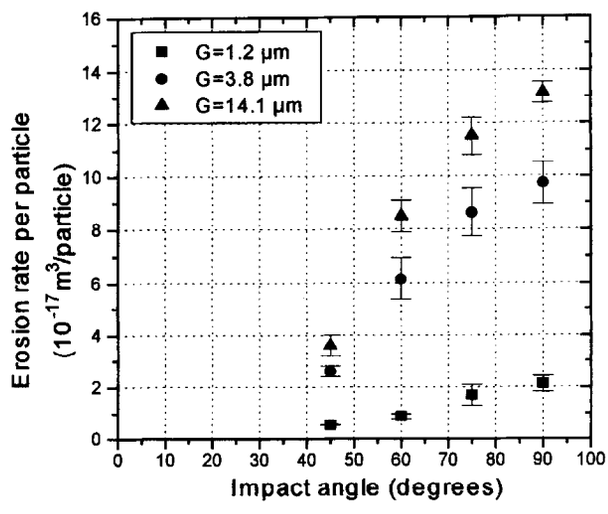

Fig. 4. Erosion rate per particle, $\Re_{mean}$, as a function of impact angle (θ).

Table 1. Variation of erosion rate with impact angle and grain size

Material	*Impact angle, θ, (degrees)*	*Eroded area, A_{imp}, ($\times 10^{-5} m^2$)*	*Weight loss, ω_{mean}, ($\times 10^{-3} g$)*	*Erosion rate, $\Re_{mean}$, ($\times 10^{-9}$ m/s)*	*Erosion rate per particle, $\Re_{mean}$, ($\times 10^{-17} m^3$ particle^{-1})*
F	45	3·70	0·15 ± 0·02	0·33 ± 0·02	0·53 ± 0·02
$G = 1{\cdot}2\,\mu m$	60	3·46	0·31 ± 0·1	0·64 ± 0·1	0·87 ± 0·1
	75	3·38	0·67 ± 0·2	1·41 ± 0·4	1·69 ± 0·4
	90	3·32	0·84 ± 0·4	1·83 ± 0·3	2·12 ± 0·3
M	45	3·70	0·81 ± 0·1	1·58 ± 0·3	2·60 ± 0·2
$G = 3{\cdot}8\,\mu m$	60	3·46	2·17 ± 0·8	4·58 ± 0·7	6·14 ± 0·8
	75	3·38	3·49 ± 0·9	7·18 ± 0·9	8·63 ± 0·9
	90	3·32	3·93 ± 0·5	8·36 ± 0·8	9·72 ± 0·8
C	45	3·70	1·13 ± 0·3	2·21 ± 0·3	3·60 ± 0·4
$G = 14{\cdot}1\,\mu m$	60	3·46	3·01 ± 0·7	6·31 ± 0·5	8·48 ± 0·6
	75	3·38	4·56 ± 0·9	9·64 ± 0·6	11·51 ± 0·7
	90	3·32	5·16 ± 0·5	11·3 ± 0·6	13·14 ± 0·4

model for erosion by brittle fracture due to normal impacts:[11]

$$E \propto r^{3\cdot7} v^{3\cdot2} \frac{\rho^{1\cdot6}}{K_{Ic}^{1\cdot3} H^{0\cdot25}} \qquad (2)$$

where v is the particle velocity normal to the surface, r and ρ are the size and density of the particle and K_{Ic} and H are the fracture toughness and hardness of the surface, respectively. The constant of proportionality differs for different assumptions, and may include other factors, such as Young's modulus, depending on the contact model used. This model cannot account for the variation of erosion rate with grain size in these alumina materials, since ρ, K_{Ic} and H are very nearly independent of grain size.

The model is based on the assumption that material is removed by the formation and intersection of lateral cracks with the surface at single impact sites. However, it is clear from our observations of eroded surfaces (Figs 1 and 2) that the main erosive process in these materials is by intersection of cracks from adjacent impacts. We are currently developing a new model of erosive wear based on the statistics of such close multiple impacts; the model and its application to experimental data such as those presented here will be reported in a further paper.

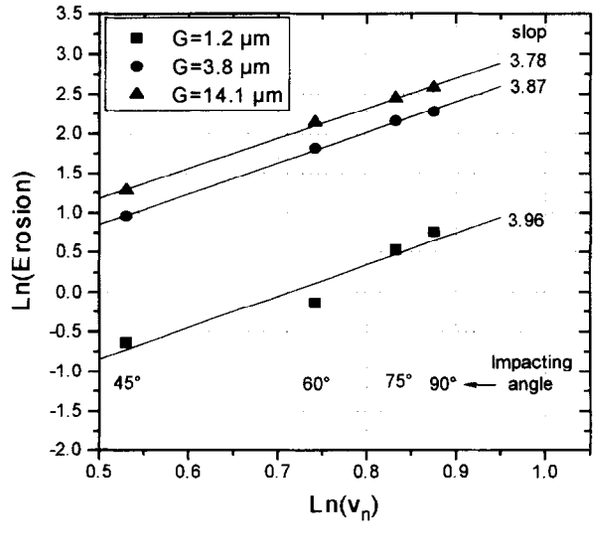

Fig. 5. Logarithm of erosion rates versus logarithm of the normal component of impact velocity, $v_n = v_{imp} \sin(\theta)$.

4 Summary and Conclusions

Polycrystalline alumina specimens, mean grain size $G = 1{\cdot}2$, 3·8 and 14·1 μm, were eroded by SiC particle impacts (at ~2·4 ms^{-1}) at incidence angles of 90°, 75°, 60° and 45°. The results may be summarised as follows:

1. the mechanism of erosive wear of the alumina used here appears to be by the interaction of the cracks associated with damaged areas from adjacent impacts;
2. the weight loss of the specimens increases linearly with test time;
3. the erosion rate is grain size dependent, being about six times greater for Al_2O_3 of 14·1 μm grain size than for 1·2 μm grain size material;
4. the erosion rate per impacting particle depends strongly on the impact angle, being three to four times higher for impacts at 90° than for impacts at 45°;
5. the variation of erosion rate with impact angle follows a power-law dependence on the normal component of the impact velocity, with an exponent of ~3·85 ± 0·1 for all grain sizes.

Acknowledgements

A. Franco thanks CAPES (Brazilian Government) for financial support. This work was also supported by the EPSRC under grant J86513.

References

1. Lawn, B. R., *Fracture of Brittle Solids*, 2nd edn. Cambridge University Press, Cambridge, UK, 1993, pp. 302–304.
2. Lawn, B. R. and Swain, M. V., Microfracture beneath point indentations in brittle solids. *J. Mater. Sci.*, 1975, **10**, 113–122.
3. Lawn, B. R. and Wilshaw, T. R., Indentation fracture: principles and applications. *J. Mater. Sci.*, 1975, **10**, 1049.
4. Evans, A. G. and Wilshaw, T. R., Dynamic solid particle damage in brittle materials: an appraisal. *J. Mater. Sci.*, 1977, **12**, 97–116.
5. Wiederhorn, S. M. and Lawn, B. R., Strength degradation of glass impacted with sharp particles: I, annealed surfaces. *J. Am. Ceram. Soc.*, 1979, **62**, 67–70.
6. Wiederhorn, S. M. and Hockey, B. J., Effect of material parameters on the erosion resistance of brittle materials. *J. Mater. Sci.*, 1983, **18**, 766–780.
7. Finnie, I., Erosion of surfaces by solid particles. *Wear*, 1960, **3**, 87–103.
8. Miranda-Martinez, M., Davidge, R. W. and Riley, F. L., Grain size effects on the wet erosive wear of high-purity polycrystalline alumina. *Wear*, 1994, **172**, 41–48.
9. Franco, A. and Roberts, S. G., Controlled wet erosive wear of polycrystalline alumina. *Journal of the European Ceramics Society*, 1996, **16**, 1365–1375.
10. Franco, A., Erosive wear of polycrystalline alumina. D. Phil thesis, University of Oxford, UK, 1996.
11. Evans, A. G., Gulden, M. E. and Rosenblatt, M. E., Impact damage in brittle materials in the elastic–plastic response regime. *Proceedings of the Royal Society (of London), Ser., A*, 1978, **361**, 343–365.